Smart Structures and Systems, Vol. 7, No. 1 (2011) 15-25
DOI: http://dx.doi.org/10.12989/sss.2011.7.1.015

Impedance-based health monitoring and mechanical testing of structures

Lizeth Vargas Palomino, Jose dos Reis Vieira de Moura Jr., Karina Mayumi Tsuruta, Domingos Alves Rade and Valder Steffen Jr.*

School of Mechanical Engineering, Federal University of Uberlandia, Campus Santa Monica, Avenida Joao Naves de Avila 2121, Bloco 1M, 38400-902 Uberlandia, Brazil

(Received September 5, 2009, Accepted August 10, 2010)

Abstract. The mechanical properties obtained from mechanical tests, such as tensile, buckling, impact and fatigue tests, are largely applied to several materials and are used today for preliminary studies for the investigation of a desired element in a structure and prediction of its behavior in use. This contribution focus on two widely used different tests: tensile and fatigue tests. Small PZT (Lead Titanate Zirconate) patches are bonded on the surface of test samples for impedance-based health monitoring purposes. Together with these two tests, the electromechanical impedance technique was performed by using aluminum test samples similar to those used in the aeronautical industry. The results obtained both from tensile and fatigue tests were compared with the impedance signatures. Finally, statistical meta-models were built to investigate the possibility of determining the state of the structure from the impedance signatures.

Keywords: structure health monitoring; electromechanical impedance; tensile tests; fatigue tests; statistical meta-modeling.

1. Introduction

Failures occurring in industrial equipment and structures in general are mostly associated to friction, fatigue, impact, and crack growth. For an appropriate functioning of a system, the failure should be located and repaired timely. In general terms, the problem of damage monitoring consists in locating and measuring the fault and estimating the system's remaining life (damage prognosis). One of the most important ambitions of modern engineering is to perform structural health monitoring in real time of structural components of high cost and considerable responsibility. Thus, the creation or improvement of techniques that enhance the accuracy and reliability of the tracking process is highly desirable and is the subject of several studies both in industry and academic environments (Farrar *et al*. 2005).

There are several techniques for monitoring the occurrence and propagation of structural damage. One of these techniques is the so-called electromechanical impedance-based structural health monitoring (Park and Inman 2005). This technique is based on the electromechanical coupling that results from a piezoelectric transducer installed on the monitored structure. Then, by measuring the electromechanical impedance, which depends on both the electrical characteristics of the transducer

*Corresponding Author, E-mail: vsteffen@mecanica.ufu.br

and the physical or mechanical characteristics of the structure (Liang *et al.* 1994), incipient damage can be detected from the variations found in the impedance curves (impedance signatures). Efforts have been made to design low cost impedance measuring systems so that traditional expensive, bulky, and power consuming impedance analyzers are no longer necessary (Grisso and Inman 2008, Finzi *et al.* 2010). Specific damage metrics can be used to quantify the damage. These damage metrics are calculated from the measurement comparisons between the cases without damage (healthy) and with damage, by using numerical and statistical tools as described in the literature (Palomino and Steffen 2009).

In contrast, the determination of mechanical properties of materials is made by performing various tests, which are usually destructive. The most widely performed tests are the following: tensile tests, bending tests, torsion tests, fatigue tests, impact tests, and compression tests. The tensile test consists of subjecting the specimen to a stretching effort, while the fatigue test is an experimental procedure that produces a permanent, progressive and localized structural damage. Fatigue test process occurs while the material is subjected to conditions that produce dynamic stresses in one or more points that can form cracks or, in some cases, cause complete failure after a sufficient number of load cycles (Branco 1994). In order to evaluate the sensitivity of the impedance-based structural health monitoring method, impedance signals were measured during tensile and fatigue testing. The impedance signatures were used to create meta-models designed to predict the stress and/or damage state of the structure.

2. Tensile and fatigue tests

The application of a force to a solid body produces a strain of the material in the direction of the load. As it is known, the tensile test consists in submitting a test sample to a tension load in the direction of its elongation.

The material does not collapse or deform permanently if the applied load is smaller than its elastic limit when the test sample is subjected to static stresses. However, when dynamic stresses are repeatedly applied to the material, collapse may occur for loads that is smaller than the maximum static load. In this case, the failure is caused by the fatigue of the material.

The behavior of a material due to fatigue depends on many factors, such as surface conditions, size and geometry of the specimen, stress concentration, stress state, temperature, type of material, and thermal treatment. The influence of each of these parameters depends on how the loading is applied to the specimen (tension, torsion, bending, etc.).

The steps that normally lead to fatigue cracks are the following: crack nucleation, crack propagation, and finally, the collapse of the test sample. The first two stages encompass most of the duration of the fatigue test and when the length of the crack is such that the cross section is sufficiently reduced, the remainder cannot resist the load and rupture occurs suddenly (Souza 2000).

The fatigue life of a specimen is given by the number of loading cycles until collapse occurs. The main types of stress cycles applied in fatigue testing can be organized according to two main groups, namely stress cycles with constant amplitude and stress cycles with varying amplitude. In the first case, the speciment is always subjected to the same stress cycle by keeping constant the force amplitude. The stress cycles with variable amplitude represent the most frequent and most difficult to analyze since both, frequency and amplitude, vary during the test (Souza 2000). The stress cycles used in the tests are the following: tension, compression and tension-compression.

3. Impedance-based structural health monitoring

The technique known as impedance-based structural health monitoring utilizes the piezoelectric properties of the PZT patch that is installed in the structure being tested and is considered as a non-destructive damage evaluation method (Park *et al*. 2003). The basic idea underlying this technique is monitoring the changes in the structure's mechanical impedance as caused by the presence of damage. Since the direct measurement of the structure's mechanical impedance is a difficult task, the method uses piezoelectric materials bonded to or incorporated into the structure, allowing the measurement of the electrical impedance. This measure is related to the structure mechanical impedance, which is affected by the presence of damage. Evidently, it is considered that the piezoelectric sensor-actuator used in the monitoring procedure remains intact along the test.

The impedance-based SHM technique was first proposed by Liang *et al.* (1994) and, subsequently, the method was extended by Chaudhry *et al.* (1995, 1996), Sun *et al.* (1995), Park *et al.* (1999, 2000, 2001, 2003), Giurgiutiu and Zagrai (2000), Giurgiutiu *et al.* (2000), Soh *et al.* (2000), Bhalla *et al.* (2002), Giurgiutiu *et al.* (2002), Moura and Steffen (2004), Peairs *et al*. (2004), Moura and Steffen (2006) and Palomino and Steffen (2009). As mentioned above, this health monitoring technique utilizes impedance sensors to monitor changes in the structural stiffness, damping and mass. The impedance sensors consist of small piezoelectric patches, usually smaller than 25×25×0.1 mm, which are used to measure directly the local dynamic response.

The piezoelectric material acts directly producing an electric voltage when a mechanical stress is applied on the material. Conversely, mechanical strains are produced when an electric field is applied. The impedance-based monitoring method uses simultaneously both versions, direct and inverse, of the piezoelectric effect (Park *et al.* 2003).

When the PZT patch is bonded to the structure and a very low electric voltage is applied, generally 1V (Raju 1997), a strain is produced in the PZT patch. Using a high frequency of excitation (in terms of typical modal analysis testing), the dynamic response of the structure is not affected by any of the following conditions: global structural modes, environment (such as flight loads), and ambient vibrations (Giurgiutiu and Zagrai 2005). Then, the response of the mechanical vibrations is transmitted to the sensor in the form of an electrical response. When an incipient damage leads to changes in the dynamic response (given by the impedance signal), this is observed in the electric response of the PZT patch.

The electromechanical model that quantifies and describes the measurement process is illustrated in Fig. 1 for a single-degree-of-freedom system.

For this system, Liang *et al.* (1994) demonstrated that the admittance $Y(\omega)$ of the PZT patch can be written as a function of the combined actuator PZT and structure mechanical impedance, as given by Eq. (1)

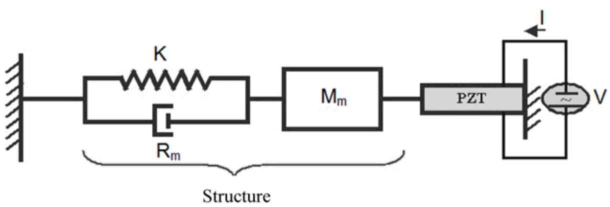

Fig. 1 Model used to represent a PZT-driven dynamic structural system

$$Y(\omega) = i\omega a\left(\bar{\varepsilon}_{33}^{T}(1 - i\delta) - \frac{Z_s(\omega)}{Z_s(\omega) + Z_a(\omega)} d_{3x}{}^{2}\hat{Y}_{xx}^{E}\right) \tag{1}$$

where $Y(\omega)$ is the electrical admittance (inverse of the impedance), $Z_a(\omega)$ and $Z_s(\omega)$ are the PZT and structure mechanical impedances, respectively. $\hat{Y}_{xx}^{E}$ is the complex Young modulus of the PZT d_{3x} is the piezoelectric coupling constant in the arbitrary x direction $\bar{\varepsilon}_{33}^{T}$ is the dielectric constant at zero stress, δ is the dielectric loss factor of the PZT, and a is a geometric constant of the PZT. Assuming that the mechanical properties of the PZT do not vary over time used for monitoring, Eq. (1) shows that the electrical impedance of the PZT patch is directly related to the structure's impedance. Damage causes changes in the structure's mechanical impedance, thus changing local dynamics features. Hence, the electrical impedance is used to monitor the structure health as represented by the structure's mechanical impedance.

The sensitivity of the technique to detect structural damage is related to the frequency range selected. A very small damage in the structure does not cause significant changes in the structure's stiffness, mass and damping properties. Hence, it is necessary for the excitation wavelength to be smaller than the characteristic length of the damage to be detected (Stokes and Cloud 1993). According to the literature, the frequency range typically used in the impedance-based method is 30 kHz to 250 kHz, although, there are other authors that have used smaller frequency ranges, such as from 10 kHz to 40 kHz (Park *et al*. 2000). The frequency range for a given structure is determined by trial and error. However, Moura and Steffen frequency (2004) presented a statistical procedure that can be used to obtain the best settings for tests of electromechanical impedance. In the impedance-based method, frequency ranges that contain several peaks of the impedance functions are usually chosen, because the number of peaks provides a better dynamic response over the frequency range. A band around a high frequency (150 kHz) is favorable to detect the location, while a lower range, around (70 kHz), covers more sensing areas (Sun *et al*. 1995). In relation to the sensitive region to identify changes, Park *et al.* (2003) claim that for a single PZT patch a damage located at a radial distance of up to 0.4 m can be identified in composite materials, and up to 2 meters in bars consisting of a single metal.

The curve that represents the impedance response provides a qualitative assessment of the damage. For a quantitative assessment of the failure, damage metrics are used (Palomino and Steffen 2009). The damage metrics used in this work is given by the average difference square metrics (Raju 1997), and its mathematical formulation is given by Eq. (2)

$$ASD = \sum_{i=1}^{n} [\mathrm{Re}(Z_{1,i}) - (\mathrm{Re}(Z_{2,i}) - \delta)]^2 \tag{2}$$

where
$$\delta = \mathrm{Re}(\bar{Z}_1) - \mathrm{Re}(\bar{Z}_2) \tag{3}$$

ASD is the average difference square metric, $\mathrm{Re}(Z_{1,i})$ is the impedance of the PZT patch measure under healthy conditions, $\mathrm{Re}(Z_{2,i})$ is the impedance for the comparison with the baseline measurement at the frequency interval i, $\mathrm{Re}(\bar{Z}_1)$ is the average value of the initial curve and $\mathrm{Re}(\bar{Z}_2)$ is the average value of the subsequent curve.

4. Fatigue tests

To determine the value of the stress amplitude that should be applied in the fatigue test so that no

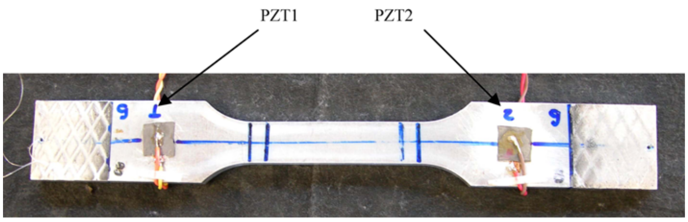

Fig. 2 PZT patches bonded on the surface of the test sample

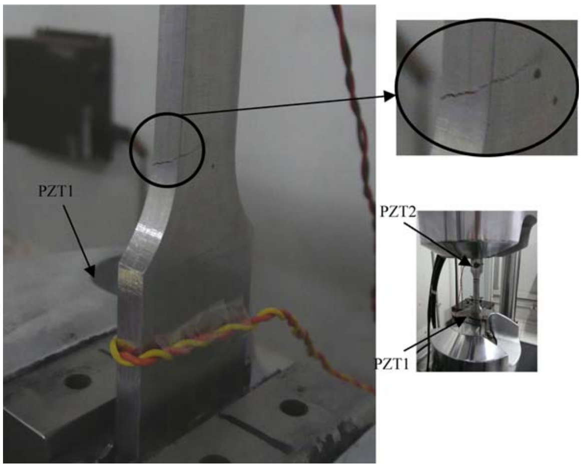

Fig. 3 Crack in the test sample (fatigue testing for the impedance-based technique)

plastic deformation results, preliminary tensile tests were done to obtain the stress-strain curve for the material used (aluminum). After determining the stress amplitude and the number of cycles, two 10×10×0.1 mm PZT patches were bonded to the test sample. The PZT patches were bonded outside the area of largest stress concentration, as shown in Fig. 2.

The test sample presented a visible crack after 50,636 cycles. Six impedance measurements were taken at each 8,000 cycles until reaching 48,000 cycles. One additional measurement was taken after the crack became visible, as shown in Fig. 3.

In summary, the procedure was as follows:

a) First, measurements were taken to determine the structural healthy state of the structure (before the fatigue testing);
b) Then, the test sample was placed in the fatigue testing machine and 8,000 force cycles were applied;
c) Impedance measurements were performed;
d) Another 8,000 cycles were applied to the specimen;
e) The sequence above was repeated until the specimen exhibited a visible crack.

Fig. 4 illustrates the procedure above.

Using the trial and error method, the best frequency range found for the present case was 39 kHz to 46 kHz. The real part of the impedance was measured for the PZT1 and PZT2 patches as shown in Fig. 5.

Considering the values of the damage metrics calculated for the two PZT patches, two meta-models with two independent variables were built, namely the damage metrics ASD PZT1 and damage metrics ASD PZT2. The dependent variable is the number of cycles. The polynomial model

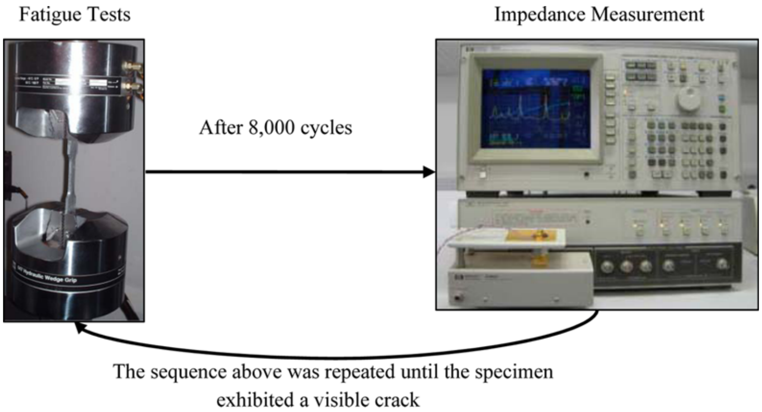

Fig. 4 The fatigue tests procedure

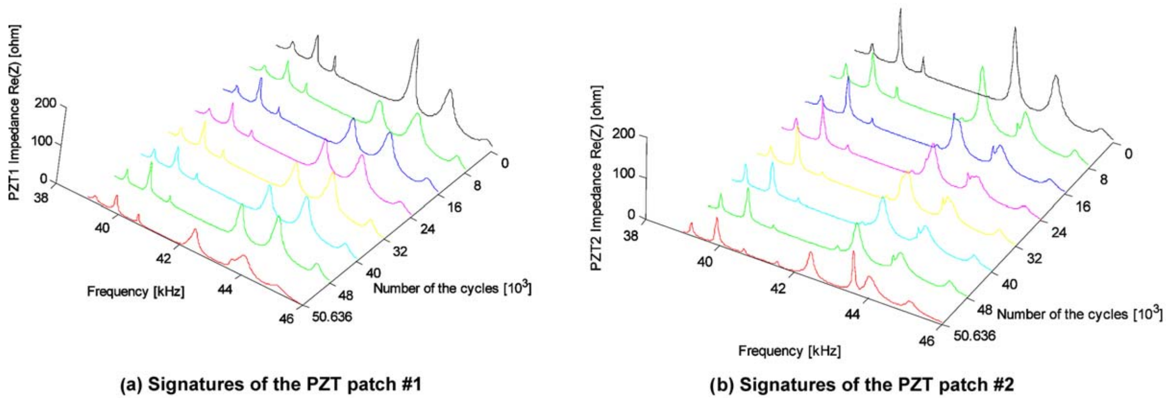

Fig. 5 Impedance signatures for the fatigue tests

adopted is given by Eq. (4).

$$\text{N}^{\circ} \text{ of cycles} = b_1 + b_2 x_1 + b_3 x_2 + b_4 x_1^2 + b_5 x_2^2 + b_6 x_1 x_2 \tag{4}$$

where x_1 is the damage metrics ASD PZT1, x_2 is the damage metrics ASD PZT2 and the values of the b_i coefficients are given below by Eq. (5).

$$\begin{bmatrix} b_1 \\ b_2 \end{bmatrix} = \begin{bmatrix} 811.028 \\ -985589.139 \end{bmatrix} \begin{bmatrix} b_3 \\ b_4 \end{bmatrix} = \begin{bmatrix} 577649.149 \\ -529230.337 \end{bmatrix} \begin{bmatrix} b_5 \\ b_6 \end{bmatrix} = \begin{bmatrix} -1051960.144 \\ 2040637.801 \end{bmatrix} \tag{5}$$

The experimental values obtained and the values calculated through the meta-model (polynomial of Eq. (4)) are shown in Fig. 6(a). It can be observed that the values obtained by the metamodel are similar to the measured values, i.e., the proposed metamodel is a good representation of the phenomenon studied. Only four false values out of 48 experiments were found (see Table 1). The corresponding response surface is depicted in Fig. 6(b). It illustrates how the metamodel mimics the real phenomenon so that all experimental points are taken into account. However, the negative values do not correspond to real experimental conditions.

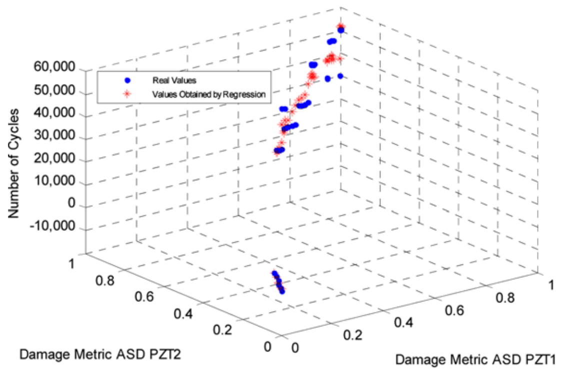

(a) Experimental values

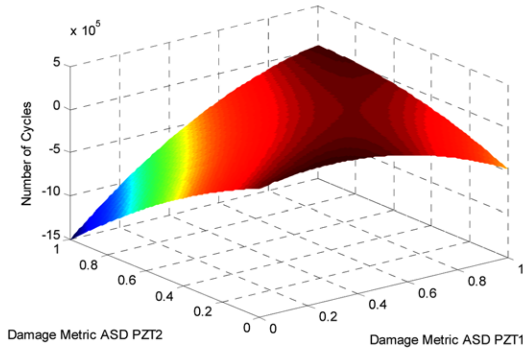

(b) Response surface

Fig. 6 Representation of the metamodel fatigue tests

Table 1 False values calculated with the metamodel

N° of measurement	N° of cycles	
	Real value	Metamodel value
13	16000	24422
35	48000	39414
36	48000	39997
41	32000	40219

If all the points had been properly classified, the model would present an adjustment of 100%. Nonetheless since the meta-model calculated four false values out of 48 experiments (Table 1), its representation was as important as 91.67% correct, which is considered satisfactory.

5. Tensile tests

For the tensile tests five ordinary test samples of aluminium were used in the experiments (Fig. 7(a)). PZT patches (10×10×0.3 mm) were bonded to one side of the test samples for monitoring purposes (Fig. 7(b)). A HP4194A impedance analyzer was used to monitor the experiments. The equipment was configured with 16 averages, 401 sampled points and with a frequency sweep from 10 to 25 kHz. This frequency range was also determined by the trial and error method. A pre-load was applied to each test sample before the experiments and the procedure followed was to acquire the real part of the impedance signature for each 0.2 mm of deformation impressed by the tensile test machine (Fig. 7(c)). Values lower than 0.6 mm as well as those subsequent to the rupture condition of the test samples were rejected since the signal was very noisy in these cases.

Differently from the fatigue tests, for the tensile tests the maximum peaks of the impedance signature in the frequency domain were used. As can be seen below, for the fatigue tests the damage metrics values were considered to extract the information of each experiment and to build a metamodel associated to the number of cycles. Here, the applied stress is directly associated to the value of frequency corresponding to the maximum peak. The reason for this is illustrated by Fig. 8.

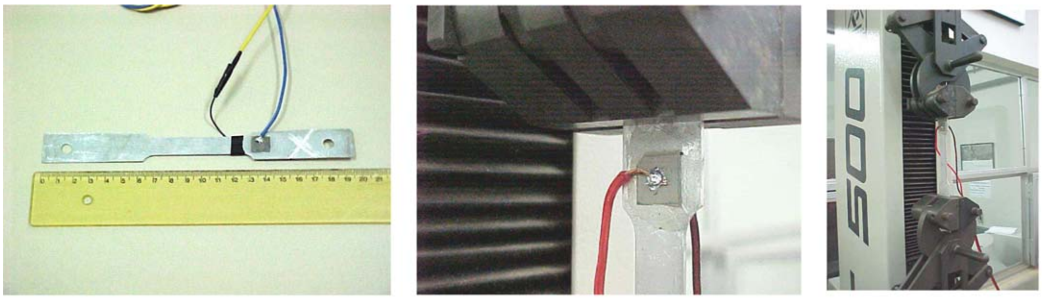

(a) Test sample (b) PZT patch detail (c) Tensile test machine

Fig. 7 Test sample used in the tensile tests

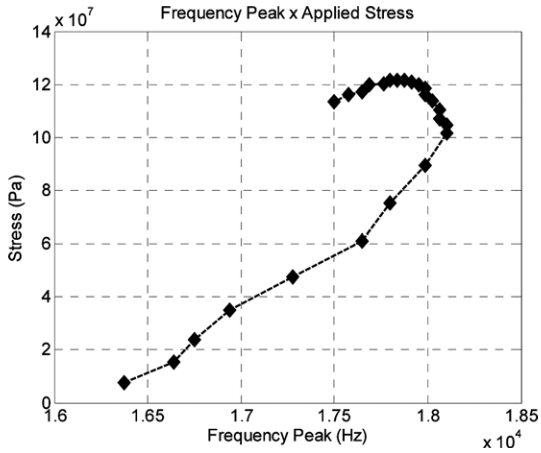

Fig. 8 Frequency peak versus applied stress for tensile tests

According to the Fig. 8, the elastic zone of the tensile tests shifts the frequency of the maximum peak to the right, while for the plastic zone the opposite occurs. A possible reason to explain this is the stress stiffening that changes the natural frequency of the specimen under an applied stress condition.

After this, a metamodel was developed for each zone to separate the different features of the tensile test. These metamodels are presented in Fig. 9.

As shown in Figs. 9(a) and 9(b), the residuals present fluctuations around zero. This means that the metamodel has no bias along the frequency lines. Consequently, the obtained metamodel is able to represent the real experiments, accordingly.

The metamodels and their corresponding representation capabilities are presented in Table 2, where $f(x)$ means the applied stress and x stands for the value of the frequency at the maximum impedance peak.

Table 2 shows statistical results regarding the quality of the metamodels obtained for the two zones considered (elastic and plastic). In particular, the values of R-square and Adjusted R-square for the two zones present good fitness (higher than 95%), meaning that the metamodels are good representations of the phenomena studied. Also, the values of RMSE (Root Mean Squared Error) for both the zones are smaller than the values of the stress itself in the metamodel, i.e., the errors do not influence the metamodels significantly.

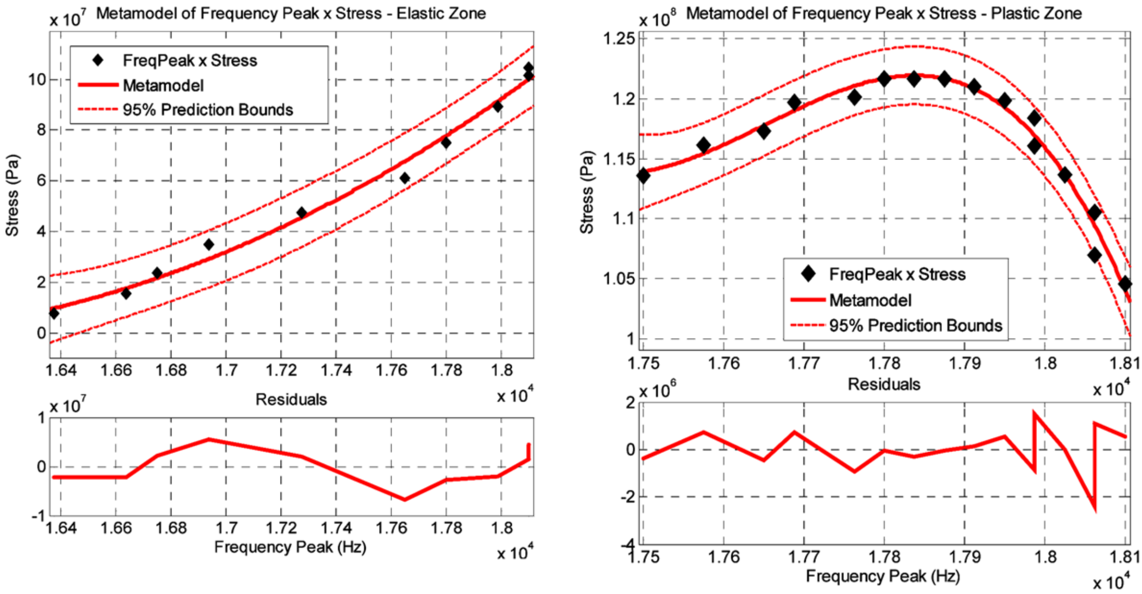

(a) Metamodel – Elastic Zone **(b) Metamodel – Plastic Zone**

Fig. 9 Metamodels for the tensile tests

Table 2 Metamodels for each zone of the tensile tests

Elastic Zone	$f(x) = 6.486{\cdot}10^6{\cdot}x^2 + 3.653{\cdot}10^7{\cdot}x + 5.028{\cdot}10^7$ Goodness of fit: SSE: $1.272{\cdot}10^{14}$ R-square: 0.9889 Adjusted R-square: 0.9858 RMSE: $4.262{\cdot}10^6$
Plastic Zone	$f(x) = -1.993{\cdot}10^6{\cdot}x^3 - 6.776{\cdot}10^6{\cdot}x^2 - 1.584{\cdot}10^6{\cdot}x + 1.219{\cdot}10^8$ Goodness of fit: SSE: $1.285{\cdot}10^{13}$ R-square: 0.9698 Adjusted R-square: 0.9622 RMSE: $1.035{\cdot}10^6$

The analysis presented above was preformed for each test sample, leading to the same behavior. However, for each test sample, the scale of applied stress related to the frequency peak varies in each case. Because of this, further studies encompassing a larger number of experiments should be performed. It should be remembered that for each material an independent study has to be done.

6. Conclusions

In the implementation of the Impedance-Based Structural Health Monitoring technique for fatigue testing, a relationship existing between the impedance measurement and the number of cycles applied to the test sample was observed. This became even more evident when the damage metrics were calculated. Finally, the damage metrics were used to create a meta-model that relates the number of cycles with the damage metrics obtained from the two PZT patches bonded on the test sample.

It is possible to conclude that a clear correlation exists between the number of cycles applied to the test samples and the impedance signals. It is believed that in a specific application it would be possible to determine the approximate fatigue life of a structural component by measuring the electromechanical impedance as shown in the present contribution. For small machine components they can be adapted to either a fatigue machine or a universal testing machine. Then, some calibration procedures are performed for the metrics used. Finally, the above methodology can be performed. However, for larger machine components, impedance based structural health monitoring can be used to evaluate the life of the structure from the impedance measurements. Further studies will be performed to confirm the above conclusions.

For the tensile tests in test samples, the behavior regarding the shifts in the maximum frequency peaks of the sampled impedance signature when stresses are applied to the structure was presented. In these experiments the difference between the two zones (the elastic and the plastic zones) is evident when monitoring the impedance signatures. A similar behavior was observed in the five experiments and the direct relationship between the impedance frequency peak and the applied stress could be observed. This is important since this concept can be used for monitoring structures under impact loading, such as gear trains, aircraft landing gears, energy cables, cranes, etc. Also, this can be used for the online monitoring of structures regarding several industrial applications. However, other tests should be done in the future to confirm the behavior above.

Acknowledgments

The authors acknowledge FINEP 01.06.1217.00/CT-AERO for the partial financing of this research work. The authors are also thankful to the Brazilian research agencies FAPEMIG and CNPq (INCT-EIE).

References

Bhalla, S., Naidu, A.S.K., Ong, C.W. and Soh, C.K. (2002), "Practical issues in the implementation of electromechanical impedance technique for NDE", *Proceedings of the SPIE International Symposium on Smart Materials, Nano-, and Micro-Smart System*, Melbourne, Australia.

Branco, C.A.G.M. (1994), *Mecânica dos Materiais*, 2nd Ed., Fundação Calouste Guelbenkian, Lisboa (in Portuguese).

Chaudhry, Z., Joseph, T., Sun, F. and Rogers, C. (1995), "Local-area health monitoring of aircraft via piezoelectric actuator/sensor patches", *Proceedings of the Smart Structures and Integrated Systems 1995*, San Diego, CA, USA.

Chaudhry, Z., Lalande, F., Ganino, A., Rogers, C.A. and Chung, J. (1996), "Monitoring the integrity of composite patch structural repair via piezoelectric actuators/sensors", *Proceedings of the 36th AIAA/ASME/ASCE/AHS/ASC Structures, Structural Dynamics, and Materials Conference and AIAA/ASME Adaptive Structures Forum. IV*, New Orleans, LA, USA.

Farrar, C.R., Lieven, N.A.J. and Bement, M.T. (2005), *Damage Prognosis for Aerospace, Civil and Mechanical System Chapter 1*, John Wiley & Sons, The Atrium, Southern Gate, West Sussex, England.

Giurgiutiu, V. and Zagrai, A. (2000), "Characterization of piezoelectric wafer active sensors", *J. Intel. Mat. Syst.*

Str., **11**(12), 959-976.
Giurgiutiu, V., Redmond, J., Roach, D. and Rackow, K. (2000), "Active sensors for health monitoring of aging aerospace structures", *Proceedings of the SPIE'S 7th International Symposium on Smart Structures and Materials and 5th International Symposium on nondestructive Evaluation and Health Monitoring of Aging Infrastructure*, Newport beach, Canada.
Giurgiutiu, V., Zagrai, A. and Bao, J.J. (2002), "Piezoelectric wafer embedded active sensors for aging aircraft structural health monitoring", *Struct. Health Monit.*, **1**(1), 41-61.
Giurgiutiu, V. and Zagrai, A. (2005), "Damage detection in thin plates and aerospace structure with the electro-mechanical impedance method", *Struct. Health Monit.,* **4**(2), 99-118.
Grisso, B. and Inman, D.J. (2008), "Autonomous hardware development for impedance-based structural health monitoring", *Smart Struct. Syst.*, **4**(3), 305-318.
Liang, C., Sun, F.P. and Rogers, C.A. (1994), "Coupled electromechanical analysis of adaptive material systems – determination of the actuator power consumption and system energy transfer", *J. Intel. Mat. Syst. Str.*, **5**(1), 12-20.
Moura, J.R.V. and Steffen, V. (2004), "Impedance-based health monitoring: frequency band evaluation", *Proceedings of the XXII IMAC International Modal Analysis Conference*, Dearborn-Michigan, USA, January .
Moura, J.R.V. and Steffen, V. (2006), "Impedance-based health monitoring for aeronautic structures using statistical meta-modeling", *J. Intel. Mat. Syst. Str.*, **17**(11), 1023-1036.
Neto R.M.F., Steffen Jr., V., Rade, D.A., Gallo, C.A. and Palomino, L.V. (2010), "A low-cost electromechanical impedance-based SHM architecture for multiplexed piezoceramic actuators", *Struct. Health Monit.,* DOI: 10.1177/1475921710379518.
Palomino, L.V. and Steffen, V. (2009), "Damage metrics associated with electromechanical impedance technique for SHM applied to a riveted structure", *Proceedings of the Cobem 2009*, Gramado-RS, Brazil.
Park, G., Kabeya, K., Cudney, H.H. and Inman, D.J. (1999), "Impedance-based structural health monitoring for temperature varying applications", *JSME Int. J. A- Solid M.*, **42**(2), 249-258.
Park, G., Cudney, H. and Inman, D.J. (2000), "An integrated health monitoring technique using structural impedance sensors", *J. Intel. Mat. Syst. Str.*, **11**(6), 448-455.
Park, G., Cudney, H. and Inman, D.J. (2001), "Feasibility of using impedance-based damage assessment for pipeline systems", *Earthq. Eng. Struct. D.*, **30**(10), 1463-1474.
Park, G., Sohn, H., Farrar, C.R. and Inman, D.J. (2003), "Overview of piezoelectric impedance-based health monitoring and path forward", *Shock Vib. Digest*, **35**(6), 85-92.
Park, G. and Inman, D.J. (2005), *Damage Prognosis for Aerospace, Civil and Mechanical System Chapter 13*, John Wiley & Sons, The Atrium, Southern Gate, West Sussex, England.
Peairs, D.M., Park, G. and Inman, D.J. (2004), "Improving accessibility of the impedance-based structural health monitoring", *J. Intel. Mat. Syst. Str.*, **15**(2), 129-139.
Raju, V. (1997), *Implementing Impedance – Based Health Monitoring*, PhD. Thesis, Virginia Polytechnic Institute and State University, Virginia.
Soh, C.K., Tseng, K., Bhalla, S. and Gupta, A. (2000), "Performance of smart piezoceramic patches in health monitoring of a RC Bridge" , *Smart Mater. Struct.*, **9**(4), 533-542.
Souza, S.A. (2000), *Ensaios mecânicos de materiais metálicos: Fundamentos teóricos e práticos*, 5th Ed., Edgard Blücher, São Paulo (in Portuguese).
Stokes, J.P. and Cloud, G.L. (1993), "The application of interferometric technique to the nondestructive inspection of fiber-reinforced materials", *Exp. Mech.,* **33**(4), 314-319.
Sun, F.P., Chaudhry, Z., Liang C. and Rogers, C.A. (1995), "Truss structure integrity identification using PZT sensor–actuator" *J. Intel. Mat. Syst. Str.*, **6**(1), 134-139.

CC